Title: Reductive samarium (electro)catalysis enabled by Sm^{III}-alkoxide protonolysis

Authors: Emily A. Boyd†, Chungkeun Shin†, David J. Charboneau, Jonas C. Peters‡*, Sarah E. Reisman‡*

5 **Affiliations:**

10

15

20

Division of Chemistry and Chemical Engineering, California Institute of Technology, Pasadena, CA, USA.

*Corresponding author. Email: jpeters@caltech.edu, reisman@caltech.edu

†These authors contributed equally to this work and are listed alphabetically.

‡These authors are listed alphabetically.

Abstract: Samarium diiodide (SmI₂) is a privileged single-electron reductant deployed in diverse synthetic settings. However, generalizable methods for catalytic turnover remain elusive due to the well-appreciated challenge associated with cleaving strong Sm^{III} $_{-}$ O bonds. Prior efforts have focused on the use of highly reactive oxophiles to enable catalyst turnover. Such approaches give rise to complex catalyst speciation and intrinsically limit the synthetic scope. Herein we leverage a mild and selective protonolysis strategy to achieve Sm-catalyzed intermolecular reductive cross-coupling of ketones and acrylates with broad scope. The modularity of our approach allows rational control of selectivity based on solvent, p K_a , and the Sm coordination sphere and provides a basis for future developments in catalytic and electrocatalytic lanthanide chemistry.

Main Text: Sm^{II} species are remarkably versatile single electron reductants. Since its introduction to synthesis by Kagan in 1977 (1), SmI₂ has become a privileged reagent (2). The lanthanide (Ln) coordination sphere is highly sensitive to Lewis basic additives which modulate both the Sm^{III/II} reduction potential and steric profile of the reagent, enabling fine control of reactivity and stereoselectivity (3,4,5). This tunability is invaluable in natural product synthesis, where stoichiometric Sm^{II} has been used to effect a variety of reductive transformations of carbonyl functional groups (see Fig. 1A for a representative example) (6,7,8,9,10,11,12). In contrast to alternative strong reductants, the compatibility of Sm^{II} species with Brønsted acids enables proton-coupled reduction reactions including conversion of dinitrogen to fixed-N products (Fig. 1A) (13,14,15,16).

5

10

15

20

25

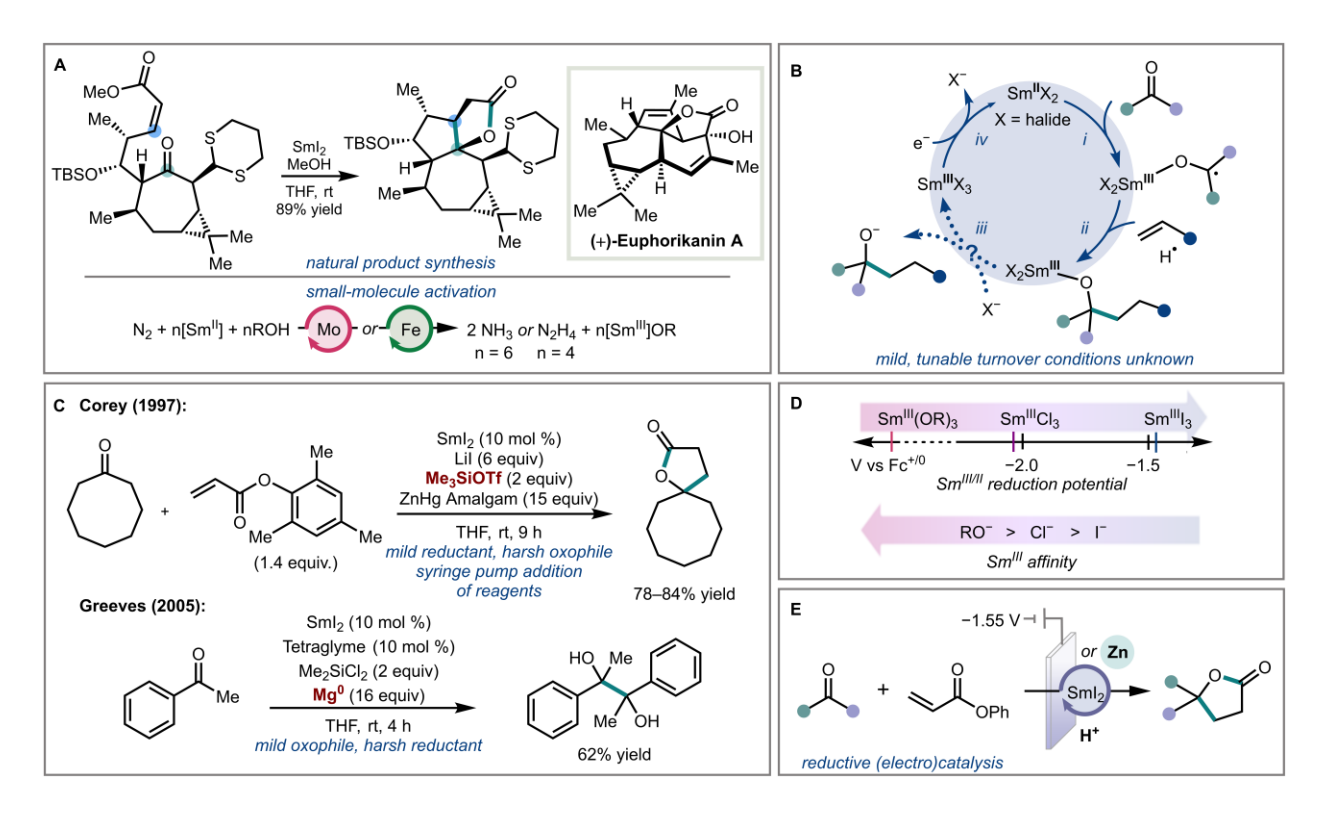


Fig. 1. Motivations and challenges associated with reductive Sm catalysis. (**A**) Utility of stoichiometric Sm^{II} reductants in diverse applications. (**B**) Targeted Sm-catalyzed cycle for ketyl-olefin coupling. (**C**) Representative Sm-catalysis precedents. (**D**) Inverse relationship between Sm^{III}—ligand affinity and reduction potential. (**E**) This work: Sm-catalyzed reductive cross-coupling of ketones and acrylates under mild chemical and electrochemical conditions.

Despite the value and versatility of Sm^{II} reductants, they are predominantly deployed (super)stoichiometrically. Additionally, SmI_2 typically must be used under dilute reaction conditions because the solubility of SmI_2 is <0.1 M in tetrahydrofuran (17). Consequently, SmI_2 is not desirable for use as a reagent in large-scale settings or early stages of multi-step synthesis. These limitations could be overcome by the development of a robust and generalizable strategy to use Sm^{II} in catalytic quantities.

The reactivity of Sm^{II} is typically driven by the high oxo- or azaphilicity that is characteristic of the f-elements (18). For example, while electron transfer (ET) from SmX₂ to ketone substrates is disfavored on the basis of outer sphere reduction potentials (step i in Fig. 1B; X = halide, $\Delta E^{\circ} > 1$

V for X = I), the strong coulombic interaction between Sm^{III} and the resulting ketyl radical anion drives such reactions forward (19). However, this stabilizing interaction presents the primary barrier to catalytic turnover (20). The cathodic reduction potentials of $Sm^{III}(OR)_n$ species are prohibitively negative for desirable catalysis (21,22,23). Exchange of OR^- with X^- to generate more readily reduced SmX_3 species is an attractive approach for turnover (steps iii and iv in Fig. 1B), but mild, selective, and tunable methods for cleavage of Sm-O bonds remain elusive.

5

10

15

20

25

30

35

40

45

The few reports that have attempted to address the challenge of reductive Sm catalysis employed halosilanes (R₃SiX) as oxophiles to cleave alkoxides from Sm^{III} (Fig. 1C) (24,25,26,27). Such methods have not been widely adopted, possibly because the reagents required for turnover have limited substrate compatibility. For instance, while relatively mild chlorosilane reagents are capable of cleaving alkoxides from Sm^{III}, exemplified by a pinacol coupling reaction reported by Greeves and coworkers (Fig. 1C), chloride rapidly displaces iodide from the Sm coordination sphere (Fig. 1D) (28). SmCl₃ is more difficult to reduce than SmI₃ and therefore requires a strong reductant such as Mg⁰. Corey and coworkers avoided the problem of halide scrambling in their Sm-catalyzed cross-coupling of ketones and acrylates by using Me₃SiOTf as an oxophile in combination with LiI (Fig. 1C); however, this required manual slow addition of Me₃SiOTf to mitigate parasitic consumption of the acrylate coupling partner. As a final point, halosilanes are not compatible with the protic additives ubiquitous in Sm^{II} chemistry (Fig. 1A).

Considering the challenge of Sm^{III}–OR turnover, we recognized that protonation would be a tunable approach to Sm–alkoxide cleavage. Here, we demonstrate rapid and reversible protonolysis of alkoxide ligands from Sm^{III} through judicious pairings of cationic Brønsted acids and halide donors. This transformation is leveraged to achieve Sm-catalyzed reductive cross-coupling of ketones and acrylates using Zn⁰ as a relatively mild source of reducing equivalents at the SmI₃/SmI₂ redox couple (Fig. 1E). Sm(OTf)₃ serves as a shelf-stable, commercially available Sm precursor and the reactions can be conducted on gram scale at ten-fold higher concentrations than is typically used when stoichiometric SmI₂ is employed (Fig. S3). The optimized conditions translate to a *bona fide* electrocatalytic system distinct from prior systems in which electrochemically driven Sm^{III/II} turnover has been difficult to firmly establish (29,30,31,32). Finally, we provide a thermochemical analysis of the factors controlling the alkoxide protonolysis step as a basis for future developments in catalytic and electrocatalytic Sm chemistry.

We began our studies by using $Sm(O^iPr)_3$ as a model of the Sm^{III} -alkoxide species generated under reductive coupling conditions, with the goal of identifying a suitable proton donor and iodide source to generate redox-active SmI_3 and enable catalysis (Fig. 2A). We anticipated that successful conditions would meet the following requirements for alkoxide–iodide exchange at Sm^{III} : i) the conjugate base of the acid should not outcompete coordination of I^- to Sm^{III} ; ii) the counterion should be chemically compatible with SmI_3/SmI_2 redox cycling (22,33); and iii) the pK_a of the acid in MeCN should be below 19, guided by the benchmarked pK_a value of 19.9 for a cationic $[Sm^{III}]^+$ complex with MeOH in MeCN (34).

Thus, we investigated a panel of acids (baseH⁺) and iodide sources and identified lutidinium bis(trifluoromethylsulfonyl)imide (LutHTFSI) as meeting these criteria, as demonstrated by cyclic voltammetry (CV). The strongly donating alkoxide ligands of Sm(OⁱPr)₃ render it redox inactive in the THF solvent window (Fig. S33). However, following addition of LutHTFSI (3.0 equiv; p K_a = 14.2 in MeCN) (35) and LiI (3 equiv) to Sm(OⁱPr)₃ in THF a quasireversible wave centered at -1.44 V vs Fc^{+/0} appeared in the CV (magenta trace in Fig. 2B), suggestive of SmI₃ generation. To verify this assignment, SmI₃ was generated through ion exchange between Sm(OTf)₃ and LiI under identical electrochemical conditions. This mixture also featured a quasireversible reduction

centered at -1.47 V (dashed blue trace). We attribute the small offset in potential to OTf-association (teal trace)). A parallel spectrophotometric experiment confirms generation of SmI₃ from Sm(OⁱPr)₃ via protonolysis/iodide substitution (Fig. S8).

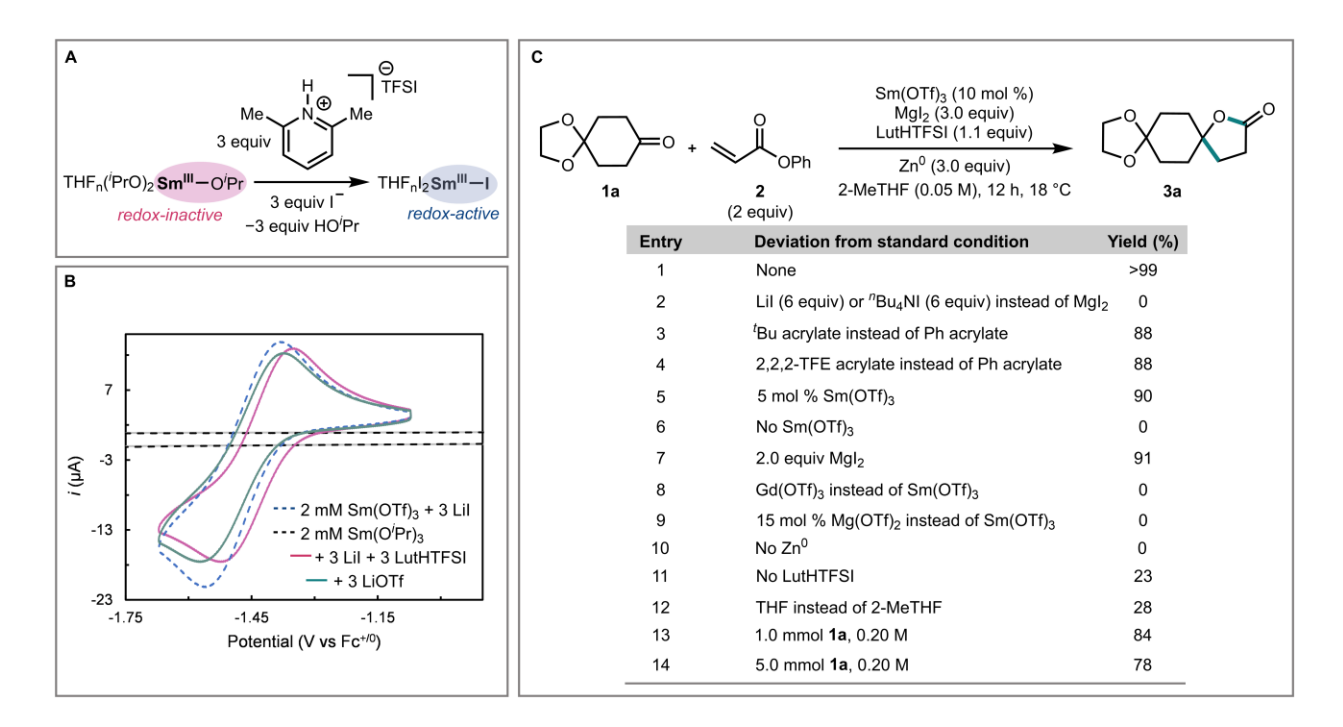


Fig. 2. Protonolysis turnover strategy and reaction development. (**A**) Proposed conversion of Sm-alkoxides to SmI₃. (**B**) CVs of 2 mM Sm(OⁱPr)₃ (black dashed trace) following the successive addition of 3 equiv each of LiI and LutHTFSI (magenta trace) and 3 equiv of LiOTf (green trace) overlaid with the CV of 2 mM Sm(OTf)₃ following addition of 3 equiv of LiI (dashed blue trace) at 100 mV s⁻¹ on a glassy carbon working electrode in THF containing 0.1 M BMPipTFSI (BMPip = 1-Butyl-1-methylpiperidinium). All potentials are referenced to Fc^{+/0} = ferrocenium/ferrocene.</sup> (**C**) Reaction optimization and control experiments conducted at 0.05 mmol scale. Listed concentrations correspond to the ketone substrate **1a**. Yields for entries 1–12 were determined by ¹H NMR spectral integration using 1,3,5-trimethoxybenzene as internal standard; entries 13–14 are isolated yields.

5

10

15

20

25

Following demonstration of this Sm-alkoxide cleavage step, we explored the reductive coupling between 1,4-cyclohexanedione monoethylene acetal (**1a**) and acrylates (R = 'Bu, CH₂CF₃, Ph) to give spirocyclic γ-lactone **3a** (36). Sm(OTf)₃ was used as an inexpensive, commercially available air-stable precatalyst. Although the CV studies used LiI as the iodide source, MgI₂ was found to be necessary for the synthetic transformation; when LiI or tetra-butylammonium iodide were used, the reactions did not change to a purple color indicative of SmI₂ in 2-MeTHF (entry 2, Fig. S2). Zn⁰ powder was selected as a mild terminal reductant. Following an initial evaluation of acrylates (R = 'Bu, CH₂CF₃, Ph; entry 3, 4), phenyl acrylate was found to perform best, furnishing γ-lactone **3a** in quantitative yield under the optimal conditions (10 mol % Sm(OTf)₃, 3.0 equiv MgI₂, 1.1 equiv LutHTFSI, 3.0 equiv Zn⁰ in 2-MeTHF (0.05 M) at 18 °C). No product was observed in the absence of Sm(OTf)₃ (entry 6), while lowering the MgI₂ loading decreased the yield slightly (entry 7). When Gd(OTf)₃ was used as a redox-inactive Lewis acid substitute for Sm(OTf)₃, no product was formed, supporting Sm^{III/II} redox activity in catalysis (entry 8). Substituting Sm(OTf)₃ with

Mg(OTf)₂ also did not furnish any product, ruling out the role of triflate in product formation (entry 9). Zn⁰ was required for product formation (entry 10), while omission of LutHTFSI resulted in low yield (entry 11). Finally, 2-methyltetrahydrofuran (2-MeTHF) as solvent performed superior to THF (entry 12).

A practical advantage of the ability to use catalytic Sm for reductive transformations is that the reactions can be performed at higher substrate concentrations. Due to the poor solubility of SmI₂ in THF, solutions of this reagent are usually prepared at concentrations of 0.1 M or lower. Indeed, the average concentration of SmI₂-mediated reactions in the literature is 0.02 M with respect to ketone (Fig. S3). Under these catalytic conditions, comparable yields of product 3a can be formed at a ten-fold higher concentration (0.20 M, Fig. 2C, entries 13 and 14), which to the best of our knowledge is the highest concentration reported for a reductive Sm transformation.

15

20

Substrate scope and demonstration of synthetic utility: The scope of the reaction is consistent with that of prior investigations (36) that employ stoichiometric SmI_2 . A variety of aliphatic and aromatic ketones performed well, giving the γ -lactone products in good to excellent yields (Fig. 3A). Common functional groups such as silyl ethers (3h), esters (3j), and aryl halides (3n–3r), sulfonates (3w), and boronate esters (3x) are compatible under the reaction conditions. Aryl ketones bearing strong electron-withdrawing substituents (3aa) resulted in lower yield due to competitive pinacol coupling. This effect is even more pronounced with 'Bu-acrylate, which further slows the rate of Giese addition relative to 2 (Fig. S10). We note that a cyclohexanone substrate bearing an α -tethered unactivated olefin exclusively formed the spirocyclic γ -lactone (3i, 3:1 dr) without any evidence of 5-exo-trig cyclization. The pharmaceutically relevant heterocyclic building blocks, tetrahydrothiopyran (3k) and tetrahydropyran (3l), were produced in synthetically useful yields.

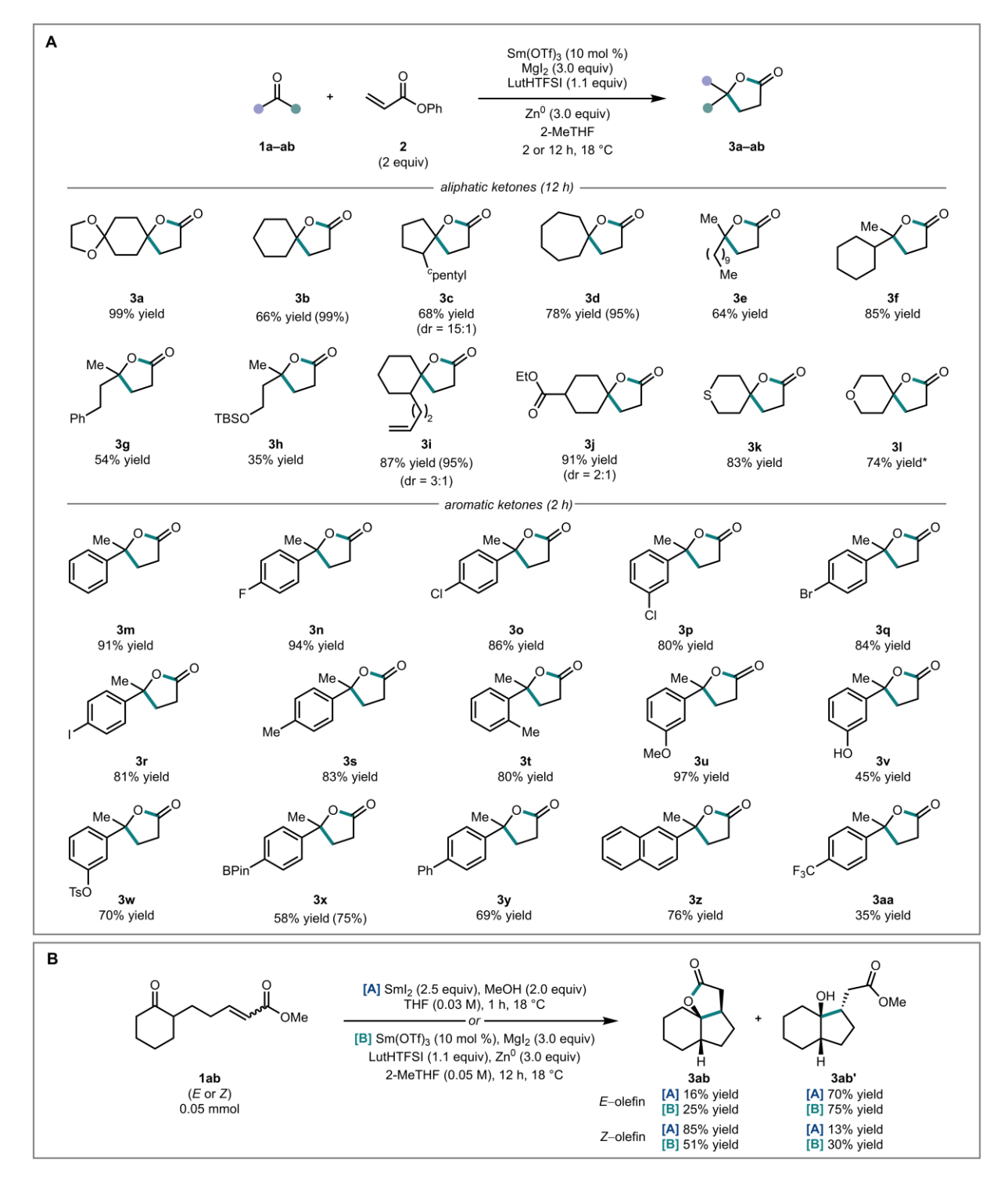


Fig. 3. Scope of Sm-catalyzed reductive cross-coupling. (**A**) Substrate scope of Sm-catalyzed reactions. Reactions conducted on a 0.3 mmol scale. Isolated yields are reported unless otherwise specified. Yields in parenthesis are determined by ¹H NMR analysis vs internal standard due to volatility of the product or instability to silica gel. *3.3 equiv LutHTFSI was used. (**B**) Intramolecular Sm-catalysis with *E*- and *Z*-1ab.

In their recent total synthesis of (+)-euphorikanin A, Carreira demonstrated that the diastereoselectivity of an intramolecular SmI_2 -mediated lactonization is dictated by the E/Z

geometry of the acrylate (6). To test if this is also true under the catalytic conditions, an analogous pair of intramolecular reductive lactonizations was performed with E- and Z-**1ab** (Fig. 3B). Using stoichiometric conditions otherwise identical to Carreria's, the cis-product was favored using the Z-olefin, while the trans-product was favored with the E-olefin. The inversion in diastereoselectivity was observed using the catalytic system, albeit with slightly diminished dr. The slight erosion in dr might result from competing Mg^{2+} ion coordination to the acrylate.

5

10

Demonstration of Electrocatalysis: Although Zn⁰ is well-suited to SmI₃/SmI₂ turnover, it is not suitable for generating Sm^{II} species with substantially more negative reduction potentials (37). Electrochemical methods, in which the applied potential can be matched to the Sm^{III/II} reduction potential, are hence appealing. However, Sm-mediated electrocatalysis is poorly developed. These reactions can suffer from competing reactivity mediated by the oxophile or metal cations generated at the sacrificial anodes; in some cases, use of a samarium metal electrode was reported as necessary (27,29,30,31,32). We sought to address these challenges by developing well-defined electrocatalysis using the samarium alkoxide protonolysis strategy discussed above.

The CV of SmI₃ generated by combining Sm(OTf)₃ and MgI₂ in 2-MeTHF features a quasireversible wave centered at -1.55 V (Fig. 4A, black trace). The CV of SmI₃ with ketone **1a**, acrylate **2**, and MgI₂ (Fig. 4A, magenta trace) exhibits an irreversible wave that is double the current intensity of the 1e⁻ reduction of SmI₃. This response, which is also observed with the aromatic ketone substrate **1m** (Fig. 4B, magenta trace), is consistent with net Sm-mediated 2e⁻ reductive coupling of the ketone and acrylate to yield a γ-alkoxy-enolate species (iii or iv, Fig. 4C).

Further addition of LutHTFSI in the presence of both ketone and acrylate gave rise to a S-shaped multielectron waves at the potential of SmI₃ reduction (Fig. 4A and B, green traces), indicative of electrocatalytic turnover. Control experiments confirm that none of the individual reaction

components (see Supplementary Materials), nor their combination in the absence of Sm (light green traces), are responsible for the current at -1.5 V.

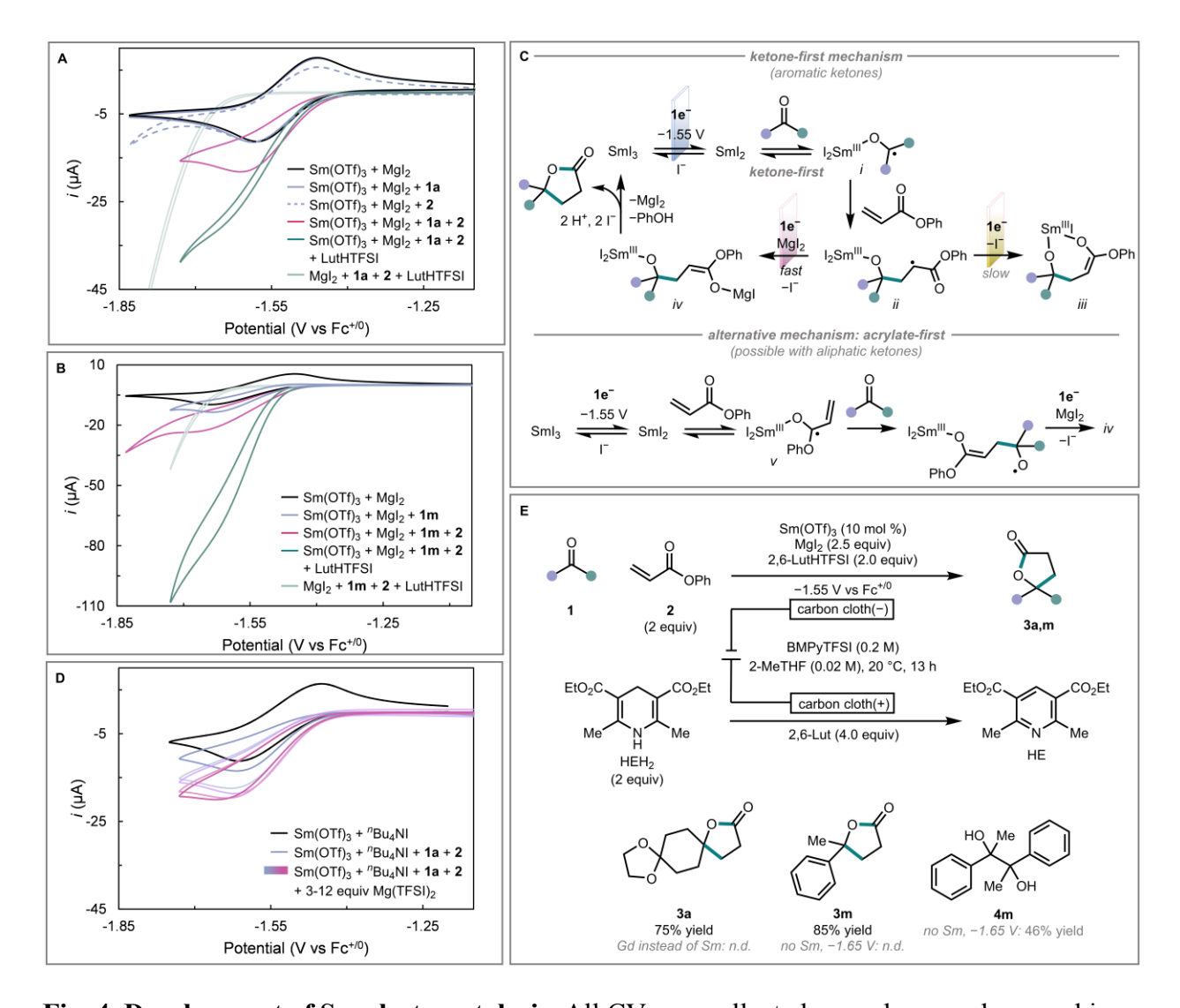


Fig. 4. Development of Sm electrocatalysis. All CVs are collected on a glassy carbon working electrode in 2-MeTHF containing 0.2 M BMPyTFSI (BMPy = 1-Butyl-1-methylpyrrolidinium) at 25 mV s⁻¹. (**A**) CVs of 2 mM Sm(OTf)₃ and MgI₂ (25 equiv, black trace) following the addition of substrates **1a** (10 equiv, solid light blue), **2** (20 equiv, dashed light blue), their combination (magenta), and the acid LutHTFSI (20 equiv, green) overlaid with the CV of the substrates, acid, and MgI₂ in the absence of Sm (light green). (**B**) CVs of 2 mM Sm(OTf)₃ and MgI₂ (25 equiv, black trace) following the addition of substrates **1m** (10 equiv, light blue), both **1m** and **2** (10 and 20 equiv, magenta), and the acid LutHTFSI (20 equiv, green) overlaid with the CV of the substrates, acid, and MgI₂ in the absence of Sm (light green). (**C**) Plausible mechanistic pathways accounting for CV responses. (**D**) CVs of 2 mM Sm(OTf)₃ and "Bu₄NI (50 equiv, black trace) following the addition of the substrates **1a** and **2** (10 and 40 equiv respectively, blue) followed by titration of Mg(TFSI)₂ (light blue-magenta traces). (**E**) CPE

5

10

conditions (0.1 mmol scale; yields determined by ¹H NMR analysis using 1,3,5-trimethoxybenzene as internal standard).

5

10

15

20

25

30

35

40

45

We also investigated the use of "Bu₄NI in place of MgI₂ to generate SmI₃ (Fig. 4D, black trace). In this case, addition of **1a** and **2** resulted in an irreversible wave with less enhancement in current relative to when MgI₂ was used (Fig. 4D, light blue trace vs. Fig 4A, magenta trace). The full 2e⁻ current is regained on titration of Mg(TFSI)₂ (light blue-magenta traces), suggesting the second electron transfer to the presumed radical intermediate (ii) at the electrode is facilitated by Mg²⁺ (38). In most stoichiometric SmI₂ reductions, every electron transferred to substrate also generates an equivalent of Lewis acidic Sm^{III}; with low concentrations of Sm, however, Mg²⁺ may alternatively stabilize alkoxide intermediates.

Substrate coupling could be initiated either by ketone reduction or acrylate reduction (Fig. 4C) (39). A "ketone-first" mechanism is likely operative with aromatic ketones such as 1m. In the CV of SmI₃ and **1m** alone, the Sm^{II} reoxidation feature completely disappears (Fig. 4B, blue trace), indicating that irreversible reduction of the aromatic ketone by SmI₂ is rapid under the electrochemical conditions. In contrast, the SmI₃/SmI₂ wave remains reversible in the presence of either (but not both) the aliphatic ketone 1a or acrylate 2 (Fig. 4A, solid and dashed light blue traces). These data indicate that the initial electron transfer step to form i or v is slow and/or uphill with these substrates (40), as is typical for the reduction of unactivated carbonyl substrates by SmI₂ (2.41). However, reduced and homocoupled products of both aliphatic ketones and acrylate 2 are observed when each substrate is subjected to the standard Zn⁰-driven catalytic conditions in the absence of the respective cross-coupling partner, suggesting that SmI2 is competent for reduction of both substrates (see Section 6.6 in the Supplementary Materials). Indeed, CVs of SmI₃ lose reversibility (Fig. S27 and S31) at increased concentrations of 1a and 2. While irreversible consumption of SmI₂ is more rapid with 2 than with 1a in this regime, electroanalytical studies suggest that the observed kinetics with 2 are an aggregate of electron transfer and homocoupling rates (see Section 8.2 in the Supplementary Materials). Without direct access to the relative rates of initial aliphatic ketone vs acrylate reduction, both "acrylate-first" and "ketone-first" mechanisms must be considered viable.

Having gained understanding of the reduction events through electroanalytical studies, we investigated electrocatalytic formation of lactone $\bf 3a$. We used constant potential electrolysis (CPE) to avoid the electrode-mediated hydrogen evolution reaction (HER) with LutHTFSI (HER onsets at approximately -1.7 V under these conditions, Fig. S21). Oxidation of Hantzsch ester (HEH₂) was selected as a well-behaved counter reaction. CPE of ketone $\bf 1a$ and acrylate $\bf 2$ with Sm(OTf)₃, LutHTFSI, and MgI₂ at an applied potential ($E_{\rm app}$) of -1.55 V (carbon cloth cathode; two-compartment cell) furnished the cross-coupled lactone $\bf 3a$ in 75% yield at 75% Faradaic efficiency (Fig. 4E). HE was produced quantitatively. Under the same conditions, phenyl-substituted lactone $\bf 3m$ was prepared in 85% yield. With this more activated substrate, current attributable to ketone reduction is observed in the absence of Sm(OTf)₃ at -1.65 V; however, under these conditions, only the pinacol product $\bf 4m$ was formed. This finding highlights the role of Sm to favor lactone formation over possible competing processes.

Thermochemistry and outlook: We also investigated the factors influencing the key proton transfer step in Sm^{III}–OR reactivation. The equilibrium of the Sm^{III} alkoxide protonolysis/ligand substitution can be decomposed into a thermochemical cycle of five components (Fig. 5A). Net protonolysis is favored by (i) a weaker affinity of the alkoxide for Sm^{III}; (ii) a higher p K_a of the corresponding alcohol; (iii) a stronger Brønsted acid (baseH⁺); (iv) a relatively weak affinity of the halide for its corresponding countercation M⁺; and (v) a stronger affinity of the halide for Sm^{III}.

Notably, the last three components are readily decoupled via independent variation of the acid, the halide donor, and the identity of the halide, enabling rational control of the net alkoxide cleavage step.

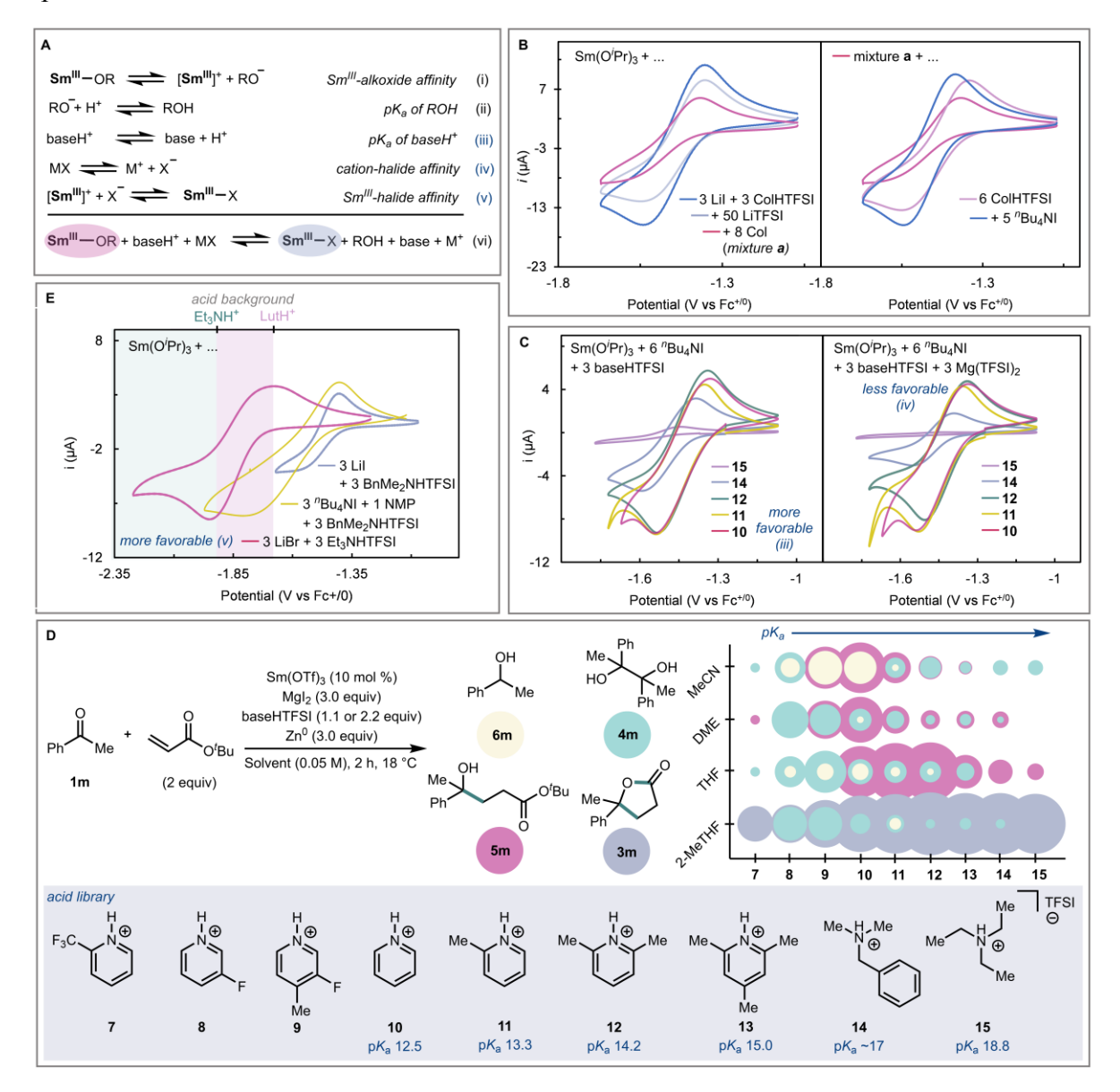


Fig. 5. Factors controlling Sm^{III}**–OR protonolysis**. All CVs are collected on a glassy carbon working electrode with 0.1 M BMPipTFSI as supporting electrolyte. (**A**) Thermochemical cycle describing Sm^{III}–OR protonolysis. (**B**) CVs demonstrating reversibility of Sm(OⁱPr)₃ (2 mM) protonolysis/iodide substitution with ColHTFSI and LiI at 100 mV s⁻¹ in THF. (**C**) CVs demonstrating the sensitivity of net protonolysis/iodide substitution to the acid p K_a and availability of iodide at 25 mV s⁻¹ in 2-MeTHF. (**D**) Product distribution of Sm-catalyzed reductive cross-coupling of acetophenone and ¹Bu-acrylate as a function of dielectric strength and acid p K_a . Diameters of circles correlate to yield of product, see Fig. S41-44 for values. (**E**)

5

CVs demonstrating the sensitivity of net protonolysis/ligand substitution to the identity of the substituting ligand at 25 mV s⁻¹ in THF.

5

10

15

20

25

30

35

40

In accord with Le Chatelier's principle (42), the amount of redox-active SmI₃ following the reaction of Sm(OⁱPr)₃ with LiI and ColHTFSI decreases with addition of LiTFSI and collidine (reflected in the CVs in Fig. 5B). The initial current intensity is restored by addition of ColHTFSI and "Bu₄NI. The influence of the p K_a of the acid (baseH⁺) was demonstrated by using "Bu₄NI as the iodide source and collecting CV data with a panel of acids spanning p K_a values of ~10 to 19. The redox activity of the system, which presumably reflects the position of the equilibrium between Sm(OⁱPr)₃ and SmI₃, decreases as the p K_a of the baseH⁺ increases (Fig. 5C). Addition of Mg cation (e.g. Mg(TFSI)₂), which has stronger affinity for I⁻ than "Bu₄N⁺, shifts the equilibrium toward Sm(OⁱPr)₃. As a result, stronger acids are required under these conditions to completely restore redox activity (compare the green vs red traces in Fig. 5C).

This relationship points to the potential breadth of the parameter space accessible for optimization of Sm-catalyzed reactions involving different substrates, intermediates, and desired products. As an illustrative example, depending on the acid and solvent used for the Sm-catalyzed coupling between **1m** and 'Bu-acrylate, different products were observed (Fig. 5D). The cross-coupled products **3m** and **5m** were favored with high pK_a acids in solvents such as THF and 2-MeTHF. A pronounced selectivity for the lactone product **3m** over its acyclic counterpart **5m** was observed in 2-MeTHF (see Supplementary Materials for details). The pinacol and reduction products **4m** and **6m** were more prevalent with low pK_a acids, particularly when strongly coordinating solvents such as acetonitrile or dimethoxyethane were used. This difference may be due to early protonolysis of the Sm^{III}-ketyl intermediate to release the neutral ketyl radical, which might rapidly dimerize or undergo reduction before productive addition to acrylate can occur (28).

The ability to tune the Sm^{III/II} redox potential by using additives with SmI₂ is an enabling feature of this reagent. For example, addition of Br⁻ generates the stronger reductant SmBr₂ (43); however, for redox cycling, an acid must be used that will protonate the Sm^{III}—alkoxide but will not undergo HER at the required potential for SmBr₃ reduction (-1.9 V). LutHTFSI is incompatible with such a strongly reducing potential. However, as the affinity of the incoming ligand for Sm^{III} increases, alkoxide cleavage becomes possible with a higher p K_a acid. The weaker acid triethylammonium (Et₃NH⁺, TFSI counteranion) meets the needed criteria to enable redox cycling of SmBr₃, giving rise to protonolysis of Sm(OⁱPr)₃ in combination with LiBr to generate SmBr₃ at a potential positive of the acid's HER background (magenta trace in Fig. 5E). Similarly, addition of the Lewis basic donor *N*-methylpyrrolidinone (NMP) results in a cathodic shift to the Sm^{III/II} couple and enhances alkoxide protonolysis with the intermediate acid BnMe₂NHTFSI (yellow trace in Fig. 5E).

These results lay the groundwork for a more generalized approach to reductive Sm catalysis and electrocatalysis under different redox regimes. Catalyst design based on incorporation of supporting ligands is of high interest, particularly with respect to developments in asymmetric Sm catalysis. While the ligand environment influences the Sm^{III/II} reduction potential, the pK_a of the acid can enable rational optimization to favor a desired Sm-catalyzed coupling over competing HER. Successive proton and electron transfer to [Sm^{III}–OR] species is also ideal for regeneration of [Sm^{II}–O(R)H] species, which can serve as potent net hydrogen atom donors. In sum, the straightforward Sm–O protonolysis strategy described herein is anticipated to enable diverse catalytic transformations, including the extension to other rare-earth elements as catalysts.

References and Notes

5

10

15

20

25

30

35

- 1. P. Girard, J. L. Namy, H. B. Kagan, Divalent lanthanide derivatives in organic synthesis. 1. Mild preparation of samarium iodide and ytterbium iodide and their use as reducing or coupling agents. *J. Am. Chem. Soc.* **102**, 2693–2698 (1980).
- 2. M. Szostak, N. J. Fazakerley, D. Parmar, D. J. Procter, Cross-coupling reactions using samarium(II) iodide. *Chem. Rev.* **114**, 5959–6039 (2014).
- 3. M. Shabangi, R. A. Flowers, Electrochemical investigation of the reducing power of SmI₂ in THF and the effect of HMPA cosolvent. *Tetrahedron Lett.* **38**, 1137–1140 (1997).
- 4. A. Dahlén, Å. Nilsson, G. Hilmersson, Estimating the limiting reducing power of SmI₂/H₂O/amine and YbI₂/H₂O/amine by efficient reduction of unsaturated hydrocarbons. *J. Org. Chem.* **71**, 1576–1580 (2006).
- 5. M. Szostak, M. Spain, D. J. Procter, Determination of the effective redox potentials of SmI₂, SmBr₂, SmCl₂, and their complexes with water by reduction of aromatic hydrocarbons. Reduction of anthracene and stilbene by samarium(II) iodide–water complex. *J. Org. Chem.* **79**, 2522–2537 (2014).
- 6. M. J. Classen, M. N. A. Böcker, R. Roth, W. M. Amberg, and E. M. Carreira, Enantioselective total synthesis of (+)-Euphorikanin A. *J. Am. Chem. Soc.* **143**, 8261–8265 (2021).
- 7. D. J. Edmonds, D. Johnston, D. J. Procter, Samarium(II)-iodide-mediated cyclizations in natural product synthesis. *Chem. Rev.* **104**, 3371-3404 (2004).
- 8. K. C. Nicolaou, S. P. Ellery, J. S. Chen, Samarium diiodide mediated reactions in total synthesis. *Angew. Chem. Int. Ed.* **48**, 7140-7165 (2009).
- 9. M. Heravi, A. Nazari, Samarium(II) iodide-mediated reactions applied to natural product total synthesis. *RSC Advances* **12**, 9944-9994 (2022).
- 10. A. K. Dey, S. Majhi, in *Rare Earth Elements*, B. Basu, B. Banerjee, Eds., (de Gruyter, 2023), ch. 7.
- 11. M. Sinast, M. Zuccolo, J. Wischnat, T. Sube, F. Hasnik, A. Baro, S. Dallavalle, S. Laschat, Samarium iodide-promoted asymmetric Reformatsky reaction of 3-(2-haloacyl)-2-oxazolidinones with enals. *J. Org. Chem.* **84**, 10050–10064 (2019).
- 12. M. Holzwarth, J. Ludwig, A. Bernz, B. Claasen, A. Majoul, J. Reuter, A. Zens, B. Pawletta, U. Bilitewski, I. M. Weiss, S. Laschat, Modulating chitin synthesis in marine algae with iminosugars obtained by SmI₂ and FeCl₃-mediated diastereoselective carbonyl ene reaction. *Org. Biomol. Chem.* **20**, 6606–6618 (2022).
- 13. N. G. Boekell, R. A. Flowers, Coordination-induced bond weakening. *Chem. Rev.* **122**, 13447–13477 (2022).
- 14. Y. Ashida, K. Arashiba, K. Nakajima, Y. Nishibayashi, Molybdenum-catalysed ammonia production with samarium diiodide and alcohols or water. *Nature* **568**, 536–540 (2019).
- 15. Y. Ashida, T. Mizushima, K. Arashiba, A. Egi, H. Tanaka, K. Yoshizawa, Y. Nishibayashi, Catalytic production of ammonia from dinitrogen employing molybdenum

- complexes bearing N-heterocyclic carbene-based PCP-type pincer ligands. *Nat. Synth*, 1–10 (2023).
- 16. E. A. Boyd, J. C. Peters, Highly selective Fe-catalyzed nitrogen fixation to hydrazine enabled by Sm(II) reagents with tailored redox potential and p K_a . *J. Am. Chem. Soc.* **145**, 14784–14792 (2023).
- 17. P. R. Chopade, T. A. Davis, E. Prasad, R. A. Flowers II, Solvent-dependent diastereoselectivities in reductions of β-hydroxyketones by SmI₂. *Org. Lett.* **6**, 2685-2688 (2004).
- 18. S. Maity, R. A. Flowers, S. Hoz, Aza versus oxophilicity of SmI₂: A break of a paradigm. *Chem. Eur. J.* **23**, 17070–17077 (2017).

5

10

15

20

25

30

35

- 19. H. Farran, S. Hoz, Quantifying the electrostatic driving force behind SmI₂ reductions. *Org. Lett.* **10**, 4875–4877 (2008).
- 20. J. C. Wedal, W. J. Evans, A rare-earth metal retrospective to stimulate all fields. *J. Am. Chem. Soc.* **143**, 18354–18367 (2021).
- 21. D. P. Halter, C. T. Palumbo, J. W. Ziller, M. Gembicky, A. L. Rheingold, W. J. Evans, K. Meyer, Electrocatalytic H₂O reduction with f-elements: mechanistic insight and overpotential tuning in a series of lanthanide complexes. *J. Am. Chem. Soc.* **140**, 2587–2594 (2018).
- 22. S. D. Ware, W. Zhang, D. J. Charboneau, C. K. Klein, S. E. Reisman, K. A. See, Electrochemical preparation of Sm(II) reagent facilitated by weakly coordinating anions. *Chem.–Eur. J.* **29**, e202301045 (2023).
- 23. R. Andreu, D. Pletcher, Ytterbium(II) as a mediator in organic electrosynthesis—possibilities and limitations. *Electrochimica Acta* **48**, 1065–1071 (2003).
- 24. E. J. Corey, G. Z. Zheng, Catalytic reactions of samarium (II) iodide. *Tetrahedron Lett.* **38**, 2045–2048 (1997).
- 25. R. Nomura, T. Matsuno, T. Endo, Samarium iodide-catalyzed pinacol coupling of carbonyl compounds. *J. Am. Chem. Soc.* **118**, 11666–11667 (1996).
- 26. H. C. Aspinall, N. Greeves, C. Valla, Samarium diiodide-catalyzed diastereoselective pinacol couplings. *Org. Lett.* **7**, 1919–1922 (2005).
- 27. L. Sun, K. Sahloul, M. Mellah, Use of electrochemistry to provide efficient SmI₂ catalytic system for coupling reactions. *ACS Catal.* **3**, 2568–2573 (2013).
- 28. S. Maity, R. A. Flowers, Mechanistic study and development of catalytic reactions of Sm(II). *J. Am. Chem. Soc.* **141**, 3207–3216 (2019).
- 29. H. Hébri, E. Duñach, M. Heintz, M. Troupel, J. Périchon, Samarium-catalyzed electrosynthesis of 1,2-diketones by the direct reductive dimerization of aromatic esters: A novel coupling reaction. *Synlett* **1991**, 901–902 (1991).
- 30. H. Hébri, E. Duñach, J. Périchon, Samarium-catalyzed electrochemical reduction of organic halides. *Synth. Commun.* **21**, 2377–2382 (1991).
- 31. B. Espanet, E. Duñach, J. Périchon, SmCl₃-catalyzed electrochemical cleavage of allyl ethers. *Tetrahedron Lett.* **33**, 2485–2488 (1992).

- 32. H. Hébri, E. Duñach, J. Périchon, SmCl₃-catalysed electrosynthesis of γ-butyrolactones from 3-chloroesters and carbonyl compounds. *J. Chem. Soc., Chem. Commun.* 499–500 (1993).
- 33. K. Arashiba, R. Kanega, Y. Himeda, Y. Nishibayashi, Electrochemical reduction of samarium triiodide into samarium diiodide. *Chem. Lett.* **49**, 1171–1173 (2020).
- 34. E. A. Boyd, J. C. Peters, Sm(II)-mediated proton-coupled electron transfer: quantifying very weak N–H and O–H homolytic bond strengths and factors controlling them. *J. Am. Chem. Soc.* **144**, 21337–21346 (2022).
- 35. S. Tshepelevitsh, A. Kütt, M. Lõkov, I. Kaljurand, J. Saame, A. Heering, P. G. Plieger, R. Vianello, I. Leito, On the basicity of organic bases in different media. *Eur. J. Org. Chem.* **2019**, 6735–6748 (2019).
- 36. S. Fukuzawa, A. Nakanishi, T. Fujinami, S. Sakai, Samarium(II) di-iodide induced reductive coupling of α,β-unsaturated esters with carbonyl compounds leading to a facile synthesis of γ-lactone. *J. Chem. Soc. Perkin Trans. 1*, 1669-1675 (1988).
- 37. M. Shabangi, J. M. Sealy, J. R. Fuchs, R. A. Flowers, The effect of cosolvent on the reducing power of SmI₂ in tetrahydrofuran. *Tetrahedron Lett.* **39**, 4429–4432 (1998).
- 38. Q.-C. Chen, S. Kress, R. Molinelli, A. Wuttig, Interfacial tuning of electrocatalytic Ag surfaces for fragment-based electrophile coupling. *Nat Catal.* 1–12 (2024).
- 39. M. Sono, S. Hanamura, M. Furumaki, H. Murai, M. Tori, First direct evidence of radical intermediates in samarium diiodide induced cyclization by ESR spectra. *Org. Lett.* **13**, 5720-5723 (2011).
- 40. J. M. Savéant, *Elements of Molecular and Biomolecular Electrochemistry* (John Wiley & Sons, 2006).
- 41. D. P. Curran, T. L. Fevig, C. P. Jasperse, M. J. Totleben, New mechanistic insights into reductions of halides and radicals with samarium(II) iodide. *Synlett*, 943-961, (1992).
- 42. H. L. Le Chatelier, *Annales des Mines* **13**, 157 (1888).

5

10

15

20

25

30

35

- 43. J. R. Fuchs, M. L. Mitchell, M. Shabangi, R. A. Flowers, The effect of lithium bromide and lithium chloride on the reactivity of SmI₂ in THF. *Tetrahedron Lett.* **38**, 8157–8158 (1997).
- 44. W. C. Still, M. Kahn, A. Mitra, Rapid chromatographic technique for preparative separations with moderate resolution. *J. Org. Chem.* **43**, 2923-2925 (1978).
- 45. J. Tu, R. A. Ripa, S. P. Kelley, M. Harmata, Intramolecular (4+3) cycloadditions of oxidopyridinium ions: Towards Daphnicyclidin A. *Chem. Eur. J.* **28**, e202200370 (2022).
- 46. X. Lei, A. Jalla, M. A. Abou Shama, J. M. Stafford, B. Cao, Chromatography-free and eco-friendly synthesis of aryl tosylates and mesylates. *Synthesis* 47, 2578-2585 (2015).
- 47. W. C. Still, C. Gennari, Direct synthesis of Z-unsaturated esters. A useful modification of the Horner-Emmons olefination. *Tetrahedron Lett.* **24**, 4405-4408 (1983).
- 48. J. A. Teprovich Jr., P. K. S. Antharjanam, E. Prasad, E. N. Pesciotta, R. A. Flowers II, Generation of Sm^{II} reductants using high intensity ultrasound. *Eur. J. Inorg. Chem.* **2008**, 5015–5019 (2008).

- 49. P. Attia, Cyclic voltammetry simulator, GitHub (2024); https://github.com/petermattia/Cyclic-Voltammetry-Simulator.
- 50. B. Hamann, J.-L. Namy, H. B. Kagan, Preparation and reactions of samarium diiodide in nitriles. *Tetrahedron* **52**, 14225-14235 (1996).
- 51. J.-L. Namy, M. Colomb, H. B. Kagan, Samarium diiodide in tetrahydropyran: Preparation and some reactions in organic chemistry. *Tetrahedron Lett.* **35**, 1723-1726 (1994).

Acknowledgments: We gratefully acknowledge Dr. Scott Virgil and the Caltech Center for Catalysis and Chemical Synthesis for access to analytical equipment, and the Dow Next Generation Educator Fund and Instrumentation Grants for their support of the EPR facility at Caltech. We also thank the Resnick Sustainability Institute at Caltech for support of enabling facilities and instrumentation.

Funding:

5

10

15

25

National Science Foundation CCI Phase II grant 2002158 (SER)

National Institutes of Health R35GM-153322 (JCP)

National Institutes of Health grant 1F32GM146439 (DJC)

National Science Foundation grant DGE-1745301 (EAB)

20 **Author contributions:**

Original conceptualization: EAB, DJC, JCP, SER.

Experimental design: CS, EAB, DJC.

Reaction optimization for chemical catalysis: CS, DJC

Electroanalytical studies, analysis, and optimization for electrocatalysis: EAB

Synthesis, scope evaluation, and compound characterization: CS.

All authors contributed to the drafting and editing of the manuscript.

Competing interests: Authors declare that they have no competing interests.

Data and materials availability: All data are available in the main text or the supplementary materials.

30 **Supplementary Materials**

Materials and Methods

Supplementary Text

Figs. S1 to S44

Tables S1 to S12

35 NMR Spectra

References (44–51)

Submitted Manuscript: Confidential Template revised November 2023